JOURNAL OF COMPUTATIONAL PHYSICS 116, 247–261 (1994)

Accurate Boundary Conditions for Multicomponent Reactive Flows

M. BAUM, T. POINSOT,* AND D. THÉVENIN†

Laboratoire d'Energétique Moléculaire et Macroscopique, Combustion, Ecole Centrale Paris, Grande Voie des Vignes, F-92295 Châtenay-Malabry, France

Received November 30, 1993

Procedures to define accurate boundary conditions for reactive flows described by Navier–Stokes equations are discussed. A formulation based on one-dimensional characteristic waves relations at the boundaries, previously developed by Poinsot and Lele for perfect gases with constant homogeneous thermodynamic properties, is rewritten and extended in order to be used in the case of gases described with realistic thermodynamic and reactive models. This kind of formulation appears to be particularly accurate and stable, which is a necessity for non-dissipative codes, in particular for direct simulation of turbulent reactive flows. The simple and solid physical basis of the method is also very attractive and makes it an easy technique to implement in any Navier–Stokes solver. Examples of application in several different computations performed with mixtures of gases and using detailed chemistry and thermodynamic modeling are described. In all cases, acoustic waves, entropy waves, and flames are proved to propagate without perturbation through the boundaries.

1. INTRODUCTION

Recent interest in full direct numerical simulations of Navier–Stokes equations, especially for reacting flows, has led to new numerical techniques and to new approaches for boundary conditions. Simulations may be performed today with high order spectral-like finite difference schemes which allow very low numerical dissipation rates [2, 3]. The precision and the potential applications of these methods, however, are constrained by the boundary conditions which have to be included in the final numerical models. Simulations in which no periodicity is assumed and flow inlets and outlets must be treated are needed for reacting flows. Indeed, these simulations are strongly dependent on boundary conditions and on their treatment, and general boundary conditions for direct simulations of compressible flows have to be developed. Although finite-difference approaches are much more flexible than spectral methods to specify boundary conditions, the choice of these conditions and the details of their numerical implementation remain difficult questions in many cases and often constitute the weakest point of the simulation.

A general method to specify boundary conditions for Navier–Stokes flows was recently derived by Poinsot and Lele [1]. This technique, called NSCBC (Navier–Stokes characteristic boundary conditions) is based on characteristic theory and includes a special treatment for viscous terms. It uses the right number of conditions to satisfy well-posedness for Euler and Navier–Stokes equations [4–6], and relaxes smoothly from Navier–Stokes to Euler conditions when the molecular viscosity goes to zero.

The NSCBC technique was derived for perfect gases with constant and homogeneous thermodynamic properties. However, direct simulations of reacting flows with complex chemistry require the treatment of gases with realistic variable thermodynamic coefficients. These variations correspond mainly to two important effects in reacting flows:

- The properties of the gas change rapidly with temperature so that even a pure gas submitted to temperature gradients will have non-constant heat capacities.
- Most gases of interest for a combustion problem are mixtures of gases and the properties of the mixture change not only because of temperature variations but also because of changes in local composition.

This paper describes how the initial NSCBC technique may be extended to consider these effects in the treatment of boundary conditions. The main difficulty considered here is to identify acoustic and entropy waves in a flow described with detailed thermodynamic models. A general technique is proposed in this paper and implemented in a reactive direct numerical simulation code.

Section 2 will describe the theory behind the method and its implementation for Navier–Stokes equations. Section 3 will provide examples of implementation for different types of boundary conditions. In Section 4, we present results obtained with this new procedure, and Section 5 will conclude the discussion.

* Present address: I.M.F.T. and C.E.R.F.A.C.S., 42 Av. G. Coriolis, F-31057 Toulouse Cedex, France.

† Present address: Institut für Technische Verbrennung, Universität Stuttgart, Pfaffenwaldring 12, D-70550 Stuttgart, Germany.

0021-9991/94 $6.00

2. MATHEMATICAL TREATMENT

2.1. *Principles of the Method*

Due to precision requirements, direct numerical simulation (DNS) techniques use centered schemes for spatial derivatives and provide only a very small amount of numerical damping. This numerical dissipation is usually too small to damp high wave-number instabilities. These numerical waves then propagate in the computational domain with group velocities which may be negative even though all physical characteristic speeds (u, $u + c$, $u - c$) may be positive [7] (as, for example, in a supersonic flow). Numerical waves are reflected at boundaries and, depending on boundary conditions, may generate new physical waves (with long wavelengths). This process leads to unphysical oscillations [1] which cannot be accepted in a DNS computation. A classical solution is to simply suppress boundary conditions by using a periodic computation domain. For reacting flows and for many practical flows with inlets and outlets, this solution is not practical and one has to deal with real boundaries. It is in this case of great importance to avoid the creation of numerical waves at boundaries and, therefore, to use carefully designed boundary conditions.

To achieve this goal, a new technique for the treatment at boundaries based on inviscid characteristic theory was introduced for the Euler equations [4, 8, 9]. An extension to Navier–Stokes cases was proposed by Poinsot and Lele [1]. The principles adopted for this extension are independent from the thermodynamic model used to describe the gas, and the procedure is performed here as described in [1]. However, the actual treatment is quite different when considering gases modeled with realistic thermodynamic properties and will be described in more detail.

The technique is based on the idea that any hyperbolic system can be associated with a corresponding system of propagating waves. At the boundaries of the computational domain, some of these waves leave the domain while others penetrate it. The outgoing waves are completely determined by the solution inside the domain and do not present any degree of freedom. On the other hand, the incoming waves cannot be fully determined unless the user has given complementary information, the so-called "boundary conditions." Determining the waves corresponding to the current problem requires a transformation between the conservative system in which the integration is generally conducted and a primitive system where the wave structures and the propagation direction of these waves, can be computed. The mathematical description proposed in this paper should help understanding the practical process and follows the lines of Thompson [4, 9]. Unfortunately, this author is working in a non-reacting case, using only one species and constant homogeneous values of all thermodynamic parameters, which leads to a quite different system of equations. Although the practical variations of these quantities are generally observed to be small, results obtained using this first theory may not be acceptable in multicomponent reacting cases (see Section 4), because of the important reflections of acoustical waves at the boundaries.

The notations employed all along this paper are analogous to those of Thompson [9] and Poinsot and Lele [1]. However, in order to use detailed chemistry modelling, it is more convenient to work in a primitive system containing the temperature in place of the pressure. All major chemistry packages (e.g., CHEMKIN and TRANSPORT [10, 11]) provide the evolution of the thermodynamic properties of the gas as a function of the temperature, and it is awkward to follow this evolution by using pressure and perfect gas law. This explains why our wave expressions will be similar but different from those used in previous publications.

Appendix A presents the mathematical derivation of the conservation equations and of the wave expression to be used at the boundaries: in order to find the characteristic waves of the conservative system under investigation, the first step is to transform it into a primitive system in which the wave structure can be easily described. Finding the eigenvalues and eigenvectors of the primitive system matrix, one can express both the primitive (A.25) and conservative systems (A.26) in terms of a vector $\mathcal{L}$ which represents the variation of the characteristic waves amplitude. The final results of Appendix A are summarized and used directly in the next section. The mathematical development of Appendix A is mainly intended for people who wish to adapt the procedure presented here to other cases (e.g., axisymmetric computation, or another system of equations). Those who work in a three-dimensional Navier–Stokes frame can readily use the results of Section 2.2 to implement this boundary treatment.

2.2. *Wave Identification in the Conservative Equations at the Boundaries*

The initial set of equations is the reactive Navier–Stokes system of conservation equations including compressibility and reaction terms for N_s different species. We define the total energy as

$$e_t = \rho \frac{u^2 + v^2 + w^2}{2} + \rho \sum_{i=1}^{N_s} (h_i Y_i) - p. \tag{1}$$

Using summation convention on indices j and k, the system of equations can be written as [12]

$$\begin{aligned}
&\frac{\partial \rho}{\partial t} + \frac{\partial (\rho u_j)}{\partial x_j} = 0 \\
&\frac{\partial (\rho u_i)}{\partial t} + \frac{\partial (\rho u_i u_j)}{\partial x_j} + \frac{\partial p}{\partial x_i} = \frac{\partial \tau_{ij}}{\partial x_j} \quad (i = 1\text{–}3) \\
&\frac{\partial e_t}{\partial t} + \frac{\partial (e_t + p) u_j}{\partial x_j} = \frac{\partial (u_j \tau_{kj})}{\partial x_k} - \frac{\partial q_j}{\partial x_j} \\
&\frac{\partial (\rho Y_i)}{\partial t} + \frac{\partial (\rho Y_i u_j)}{\partial x_j} = - \frac{\partial (\rho Y_i V_{D,i,j})}{\partial x_j} + W_i \dot{\omega}_i \quad (i = 1\text{–}N_s).
\end{aligned} \tag{2}$$

The pressure can then be computed using the perfect gas law:

$$p = \rho r T. \tag{3}$$

The final outcome of the analysis of Appendix A is to provide an equivalent form of these equations in which characteristic waves are easily identified (A.26). From now on, we will consider only the boundary conditions associated with the x direction (boundaries corresponding to a constant x value). Results for y and z boundaries are fully symmetrical. In non-conservative form, the final set of equations is, when developing (A.25):

$$\begin{aligned}
&\frac{\partial \rho}{\partial t} + \frac{\rho \overline{C}_p}{c^2}(\mathcal{L}_1 + \mathcal{L}_{N_s+5}) + \mathcal{L}_{N_s+4} + C_1 = 0\\
&\frac{\partial T}{\partial t} + \mathcal{L}_1 + \mathcal{L}_{N_s+5} + \sum_{i=4}^{N_s+3} \mathcal{L}_i + C_2 = 0\\
&\frac{\partial u}{\partial t} + (\mathcal{L}_{N_s+5} - \mathcal{L}_1)\frac{\overline{C}_p}{c} + C_3 = 0\\
&\frac{\partial v}{\partial t} + \mathcal{L}_2 + C_4 = 0\\
&\frac{\partial w}{\partial t} + \mathcal{L}_3 + C_5 = 0\\
&\frac{\partial Y_1}{\partial t} - \frac{W_1}{\overline{W}}\frac{1}{T}\mathcal{L}_4 - \frac{W_1}{\overline{W}}\frac{1}{\rho}\mathcal{L}_{N_s+4} + C_6 = 0\\
&\frac{\partial Y_2}{\partial t} - \frac{W_2}{\overline{W}}\frac{1}{T}\mathcal{L}_5 + C_7 = 0\\
&\qquad\vdots\\
&\frac{\partial Y_{N_s}}{\partial t} - \frac{W_{N_s}}{\overline{W}}\frac{1}{T}\mathcal{L}_{N_s+3} + C_{N_s+5} = 0.
\end{aligned} \tag{4}$$

Most codes for compressible flows use a conservative form for these equations. In this case, the system to use is (after developing (A.26)):

$$\begin{aligned}
&\frac{\partial \rho}{\partial t} + \frac{\rho \overline{C}_p}{c^2}(\mathcal{L}_1 + \mathcal{L}_{N_s+5}) + \mathcal{L}_{N_s+4} + \tilde{C}_1 = 0\\
&\frac{\partial e_t}{\partial t} + \left(\frac{u^2+v^2+w^2}{2} + \sum_{i=1}^{N_s} h_i Y_i\right)\left[\frac{\rho \overline{C}_p}{c^2}(\mathcal{L}_1 + \mathcal{L}_{N_s+5}) + \mathcal{L}_{N_s+4}\right]\\
&\quad + pu\frac{\overline{C}_p}{c}(\mathcal{L}_{N_s+5} - \mathcal{L}_1) + \rho v \mathcal{L}_2 + \rho w \mathcal{L}_3\\
&\quad + \rho \sum_{i=1}^{N_s}\left[\left(\overline{C}_p - \frac{h_i W_i}{\overline{W}T}\right)\mathcal{L}_{i+3}\right] - \frac{h_1 W_1}{\overline{W}}\mathcal{L}_{N_s+4} + \tilde{C}_2 = 0\\
&\frac{\partial(\rho u)}{\partial t} + \frac{\rho \overline{C}_p}{c^2}(u-c)\mathcal{L}_1 + \frac{\rho \overline{C}_p}{c^2}(u+c)\mathcal{L}_{N_s+5} + u\mathcal{L}_{N_s+4} + \tilde{C}_3 = 0\\
&\frac{\partial(\rho v)}{\partial t} + \frac{\rho v \overline{C}_p}{c^2}(\mathcal{L}_1 + \mathcal{L}_{N_s+5}) + \rho \mathcal{L}_2 + v\mathcal{L}_{N_s+4} + \tilde{C}_4 = 0\\
&\frac{\partial(\rho w)}{\partial t} + \frac{\rho w \overline{C}_p}{c^2}(\mathcal{L}_1 + \mathcal{L}_{N_s+5}) + \rho \mathcal{L}_3 + w\mathcal{L}_{N_s+4} + \tilde{C}_5 = 0\\
&\frac{\partial(\rho Y_1)}{\partial t} + \frac{\rho Y_1 \overline{C}_p}{c^2}(\mathcal{L}_1 + \mathcal{L}_{N_s+5}) - \frac{W_1}{\overline{W}}\frac{\rho}{T}\mathcal{L}_4 + \left(Y_1 - \frac{W_1}{\overline{W}}\right)\mathcal{L}_{N_s+4} + \tilde{C}_6 = 0\\
&\frac{\partial(\rho Y_j)}{\partial t} + \frac{\rho Y_j \overline{C}_p}{c^2}(\mathcal{L}_1 + \mathcal{L}_{N_s+5}) - \frac{W_j}{\overline{W}}\frac{\rho}{T}\mathcal{L}_{j+3} + Y_j\mathcal{L}_{N_s+4} + \tilde{C}_{j+5} = 0.
\end{aligned} \tag{5}$$

In these systems, the C_i's defined in (A.19) take into account all terms which do not involve any first derivative of the primitive variables vector U (A.2) along the x direction, i.e., the viscous, diffusive, and reactive parts. This form is the generalization to reactive gases with variable thermodynamic properties of the initial equations of Poinsot and Lele (Eqs. (24) to (28) in [1]).

In this set of equations, the $\mathcal{L}_j$ terms are wave amplitude variations and can be written, for $j = 2$ to N_s:

$$\mathcal{L}_1 = (u-c)\left[\left(\frac{1}{2}\frac{\gamma-1}{\gamma}\frac{T}{\rho}\right)\frac{\partial \rho}{\partial x} + \left(\frac{1}{2}\frac{\gamma-1}{\gamma}\right)\frac{\partial T}{\partial x} - \left(\frac{1}{2}\frac{c}{\overline{C}_p}\right)\frac{\partial u}{\partial x} + \sum_{i=1}^{N_s}\left(\frac{1}{2}\frac{\gamma-1}{\gamma}\frac{\overline{W}T}{W_i}\right)\frac{\partial Y_i}{\partial x}\right] \tag{6}$$

$$\mathcal{L}_2 = u\frac{\partial v}{\partial x} \tag{7}$$

$$\mathcal{L}_3 = u\frac{\partial w}{\partial x} \tag{8}$$

$$\mathcal{L}_4 = u\left[\left(\frac{1-\gamma}{\gamma}\frac{T}{\rho}\right)\frac{\partial \rho}{\partial x} + \left(\frac{1}{\gamma}\right)\frac{\partial T}{\partial x} - \left(\frac{\overline{W}T}{W_1}\right)\frac{\partial Y_1}{\partial x} + \sum_{i=1}^{N_s}\left(\frac{1}{\gamma}\frac{\overline{W}T}{W_i}\right)\frac{\partial Y_i}{\partial x}\right] \tag{9}$$

$$\mathcal{L}_{j+3} = u\left[-\left(\frac{\overline{W}T}{W_j}\right)\frac{\partial Y_j}{\partial x}\right] \tag{10}$$

$$\mathcal{L}_{N_s+4} = u\left[\left(\frac{\gamma-1}{\gamma}\right)\frac{\partial \rho}{\partial x} - \left(\frac{\rho}{\gamma T}\right)\frac{\partial T}{\partial x} - \sum_{i=1}^{N_s}\left(\frac{\overline{W}}{W_i}\frac{\rho}{\gamma}\right)\frac{\partial Y_i}{\partial x}\right] \tag{11}$$

$$\mathcal{L}_{N_s+5} = (u+c)\left[\left(\frac{1}{2}\frac{\gamma-1}{\gamma}\frac{T}{\rho}\right)\frac{\partial \rho}{\partial x} + \left(\frac{1}{2}\frac{\gamma-1}{\gamma}\right)\frac{\partial T}{\partial x} + \left(\frac{1}{2}\frac{c}{\overline{C}_p}\right)\frac{\partial u}{\partial x} + \sum_{i=1}^{N_s}\left(\frac{1}{2}\frac{\gamma-1}{\gamma}\frac{\overline{W}T}{W_i}\right)\frac{\partial Y_i}{\partial x}\right]. \tag{12}$$

The wave speeds associated to the different $\mathcal{L}_i$'s are respectively

$(u - c)$ for $\mathcal{L}_1$, u for all $\mathcal{L}_j$'s with $j = 2$ to $(N_s + 4)$, and $(u + c)$ for $\mathcal{L}_{N_s+5}$.

2.3. *Wave Specification Using the Extended NSCBC Technique*

Up to now, we only replaced an expression (the convective derivatives) in the primitive system of equations by an equal value expressed in terms of the characteristic waves of this system. The next step is to determine the characteristic waves whose value will change depending on the chosen boundary conditions.

In the NSCBC method, this is done by assuming that the waves at the boundaries in the full Navier–Stokes problem have the same amplitude as in the case of an inviscid one-dimensional problem. The analysis is then performed by considering the equations corresponding to this local one-dimensional inviscid non-reacting associated system (LODI system). At the boundaries of the computational domain ($x = x_{\min}$ or $x = x_{\max}$ for the x direction), the system (4) is rewritten under the assumption of negligible viscous, reactive, and transverse terms (i.e., the C_i terms are neglected) to obtain the LODI relations. These LODI relations provide "compatibility" conditions between the values of the $\mathcal{L}_i$'s and the conditions used at the boundary. In terms of non-conservative variables, the LODI equations are:

$$\frac{\partial \rho}{\partial t} + \frac{\rho \overline{C}_p}{c^2}(\mathcal{L}_1 + \mathcal{L}_{N_s+5}) + \mathcal{L}_{N_s+4} = 0 \tag{13}$$

$$\frac{\partial T}{\partial t} + \mathcal{L}_1 + \mathcal{L}_{N_s+5} + \sum_{i=4}^{N_s+3} \mathcal{L}_i = 0 \tag{14}$$

$$\frac{\partial u}{\partial t} + (\mathcal{L}_{N_s+5} - \mathcal{L}_1)\frac{\overline{C}_p}{c} = 0 \tag{15}$$

$$\frac{\partial v}{\partial t} + \mathcal{L}_2 = 0 \tag{16}$$

$$\frac{\partial w}{\partial t} + \mathcal{L}_3 = 0 \tag{17}$$

$$\frac{\partial Y_1}{\partial t} - \frac{W_1}{\overline{W}}\frac{1}{T}\mathcal{L}_4 - \frac{W_1}{\overline{W}}\frac{1}{\rho}\mathcal{L}_{N_s+4} = 0 \tag{18}$$

$$\frac{\partial Y_2}{\partial t} - \frac{W_2}{\overline{W}}\frac{1}{T}\mathcal{L}_5 = 0 \tag{19}$$

$$\vdots$$

$$\frac{\partial Y_{N_s}}{\partial t} - \frac{W_{N_s}}{\overline{W}}\frac{1}{T}\mathcal{L}_{N_s+3} = 0. \tag{20}$$

LODI conditions may be obtained for all variables of interest so that any boundary condition will have a corresponding LODI condition relating wave amplitudes variations. For example, LODI relations associated to pressure, flow rate, or total enthalpy are:

$$\frac{\partial p}{\partial t} + \rho \overline{C}_p(\mathcal{L}_1 + \mathcal{L}_{N_s+5}) = 0 \tag{21}$$

$$\frac{\partial(\rho u)}{\partial t} + \frac{\rho \overline{C}_p}{c}\left[(\mathcal{L}_{N_s+5} - \mathcal{L}_1) + \frac{u}{c}(\mathcal{L}_1 + \mathcal{L}_{N_s+5})\right] + u\mathcal{L}_{N_s+4} = 0 \tag{22}$$

$$\frac{\partial h_t}{\partial t} + \overline{C}_p(\mathcal{L}_1 + \mathcal{L}_{N_s+5}) + \frac{u\overline{C}_p}{c}(\mathcal{L}_{N_s+5} - \mathcal{L}_1) + v\mathcal{L}_2 + w\mathcal{L}_3 + \sum_{i=1}^{N_s}\left[\left(\overline{C}_p - \frac{h_i W_i}{\overline{W}T}\right)\mathcal{L}_{i+3}\right] - \frac{h_1 W_1}{\overline{W}\rho}\mathcal{L}_{N_s+4} = 0. \tag{23}$$

Moreover, it is also straightforward to derive LODI relations associated to gradients:

$$\begin{aligned}
\frac{\partial \rho}{\partial x} &= \frac{\rho \overline{C}_p \mathcal{L}_1}{c^2(u-c)} + \frac{\rho \overline{C}_p \mathcal{L}_{N_s+5}}{c^2(u+c)} + \frac{\mathcal{L}_{N_s+4}}{u} \\
\frac{\partial T}{\partial x} &= \frac{\mathcal{L}_1}{u-c} + \frac{\mathcal{L}_{N_s+5}}{u+c} + \frac{1}{u}\sum_{i=1}^{N_s}\mathcal{L}_{i+3} \\
\frac{\partial u}{\partial x} &= \frac{\overline{C}_p}{c}\left(\frac{\mathcal{L}_{N_s+5}}{u+c} - \frac{\mathcal{L}_1}{u-c}\right) \\
\frac{\partial v}{\partial x} &= \frac{\mathcal{L}_2}{u} \\
\frac{\partial w}{\partial x} &= \frac{\mathcal{L}_3}{u} \\
\frac{\partial Y_1}{\partial x} &= -\frac{W_1}{\overline{W}u}\left(\frac{\mathcal{L}_4}{T} + \frac{\mathcal{L}_{N_s+4}}{\rho}\right) \\
\frac{\partial Y_i}{\partial x} &= -\frac{W_i}{\overline{W}Tu}\mathcal{L}_{i+3} \quad (i = 2\text{–}N_s) \\
\frac{\partial p}{\partial x} &= \rho \overline{C}_p\left(\frac{\mathcal{L}_1}{u-c} + \frac{\mathcal{L}_{N_s+5}}{u+c}\right).
\end{aligned} \tag{24}$$

The LODI relations are used to infer values for the $\mathcal{L}_i$ terms so that these values are compatible with the desired boundary conditions. Note that the final set of equations which will be used to integrate boundary values in time is not the LODI system but system (4) or (5) which involve all terms (transverse, viscous, and reaction terms). The LODI system is only invoked to provide wave amplitude estimations at the boundaries. For example, if we want to impose a constant x-velocity at the boundary, we see from (15) that we should impose $\mathcal{L}_{N_s+5} = \mathcal{L}_1$. A complete discussion of these relations can be found in [1]. In particular, conditions corresponding to the viscous part of the equations are given in [1] and were used without changes here.

Some examples of implementation are given for the new procedure in the next section, including the "non-reflecting" and inlet conditions used for the computations presented in Section 4.

3. PRACTICAL IMPLEMENTATION

The practical use of the proposed boundary treatment is simple and can be described in four points:

1. Inside the domain, time-integration is realized as usual.

2. At each boundary, the sign of the eigenvalues associated to the different $\mathcal{L}_i$'s is determined. The $\mathcal{L}_i$'s associated with outflowing waves are determined from the solution inside the computational domain, and may be computed by using appropriate equations (6) to (12). The gradients appearing in (6) to (12) are derived from one-sided derivatives inside the computational domain.

3. Generally (except for supersonic flows), not all eigenvalues have the same sign. This means that some $\mathcal{L}_i$'s are still undetermined after the previous step because they correspond to ingoing waves. These $\mathcal{L}_i$'s cannot be computed from values of the solution inside the domain. They have to be obtained from the appropriate LODI equations given in (13) to (20).

4. After all $\mathcal{L}_i$'s are known at the boundaries, their values are used for the time-integration, considering (4) in primitive variables, or (5) in conservative form. The C_i's or $\tilde{C}_i$'s are computed in the same way as inside the domain, but with one-sided derivatives as the solution is only known on one side of the boundary. At this level, specific Navier–Stokes conditions are integrated if necessary as described in [1].

Let us now consider some usual boundary conditions:

• Subsonic inlet with imposed values. The values of the $\mathcal{L}_i$'s that might be imposed are given by (14) to (20) in the LODI system of equations. For example, $\mathcal{L}_{N_s+5} = \mathcal{L}_1$ is the compatibility condition to impose if one wants to see the inlet x-velocity at a constant value, corresponding to the local initial condition. In the same way, $\mathcal{L}_2 = \mathcal{L}_3 = 0$ corresponds to a constant y and z-velocity at the inlet. Letting $\mathcal{L}_i = 0$ for $i = 5$ to $N_s + 3$ corresponds to imposed mass fractions Y_2 to Y_{N_s}. The condition $\mathcal{L}_4 = -(T/\rho)\mathcal{L}_{N_s+4}$ is required if Y_1 is to be imposed. If the temperature is to be imposed: $2\mathcal{L}_1 + \sum_{i=4}^{N_s+3} \mathcal{L}_i = 0$.

Considering again all these conditions, it can be seen that such a subsonic inflow possesses only one degree of freedom, which was expected as only one eigenvalue $(u - c)$ is negative at this boundary. This eigenvalue is associated with $\mathcal{L}_1$, which means that $\mathcal{L}_1$ is directly computed from the solution inside the computational domain and can be used to compute all the other $\mathcal{L}_i$'s, with the system being written finally:

$$\mathcal{L}_1 = (u - c)\left[\left(\frac{1}{2}\frac{\gamma - 1}{\gamma}\frac{T}{\rho}\right)\frac{\partial \rho}{\partial x} + \left(\frac{1}{2}\frac{\gamma - 1}{\gamma}\right)\frac{\partial T}{\partial x} - \left(\frac{1}{2}\frac{c}{\overline{C}_p}\right)\frac{\partial u}{\partial x} + \sum_{i=1}^{N_s}\left(\frac{1}{2}\frac{\gamma - 1}{\gamma}\frac{\overline{W}T}{W_i}\right)\frac{\partial Y_i}{\partial x}\right]$$

$$\begin{aligned}
\mathcal{L}_2 &= 0 \\
\mathcal{L}_3 &= 0 \\
\mathcal{L}_4 &= -2\mathcal{L}_1 \\
\mathcal{L}_5 &= 0 \\
&\vdots \\
\mathcal{L}_{N_s+3} &= 0 \\
\mathcal{L}_{N_s+4} &= 2\frac{\rho}{T}\mathcal{L}_1 \\
\mathcal{L}_{N_s+5} &= \mathcal{L}_1 .
\end{aligned} \tag{25}$$

• Supersonic outflow. In this case, all the eigenvalues are positive, which means for an outflow that all $\mathcal{L}_i$'s are directly computed by using values inside the computational domain, as all waves are leaving this domain. No additional boundary conditions are required.

• Subsonic non-reflecting outflow. In this case, only one eigenvalue is negative. For an outgoing flow, this means that there is only one degree of freedom, as in the first case considered above. It would be possible to get a perfectly "non-reflecting" system by setting $\mathcal{L}_1 = 0$. In fact, as explained in [1], such a perfectly non-reflecting system is generally irrelevant. This condition (see [9]) can lead to serious problems. Considering, for example, a two-dimensional shear layer, using at the inlet the conditions described above for a subsonic inflow and implementing at all other boundaries perfectly non-reflecting conditions would impede the determination of an average value of the pressure in the computational domain. Physically, this information is provided by pressure waves coming from downstream "infinity" and propagating upstream. In this particular case, perfectly non-reflecting conditions lead to an ill-posed problem. Having recognized this fact, it is possible to model the physical information process by letting small acoustical waves feed pressure information back into the domain through the downstream boundary, by imposing [1]

$$\mathcal{L}_1 = K(p - p_\infty); \tag{26}$$

TABLE I

Conditions of the Different Test Cases

Figure	Wave type	Wave direction	Boundary type	Method
1	Acoustic	Right	Non-reflecting	[1]
2	Acoustic	Right	Non-reflecting	This paper
3	Acoustic	Left	Inlet	This paper
4	Entropy	Right	Non-reflecting	This paper
6–9	Natural	Both	Inlet ↔ Non-reflecting	This paper

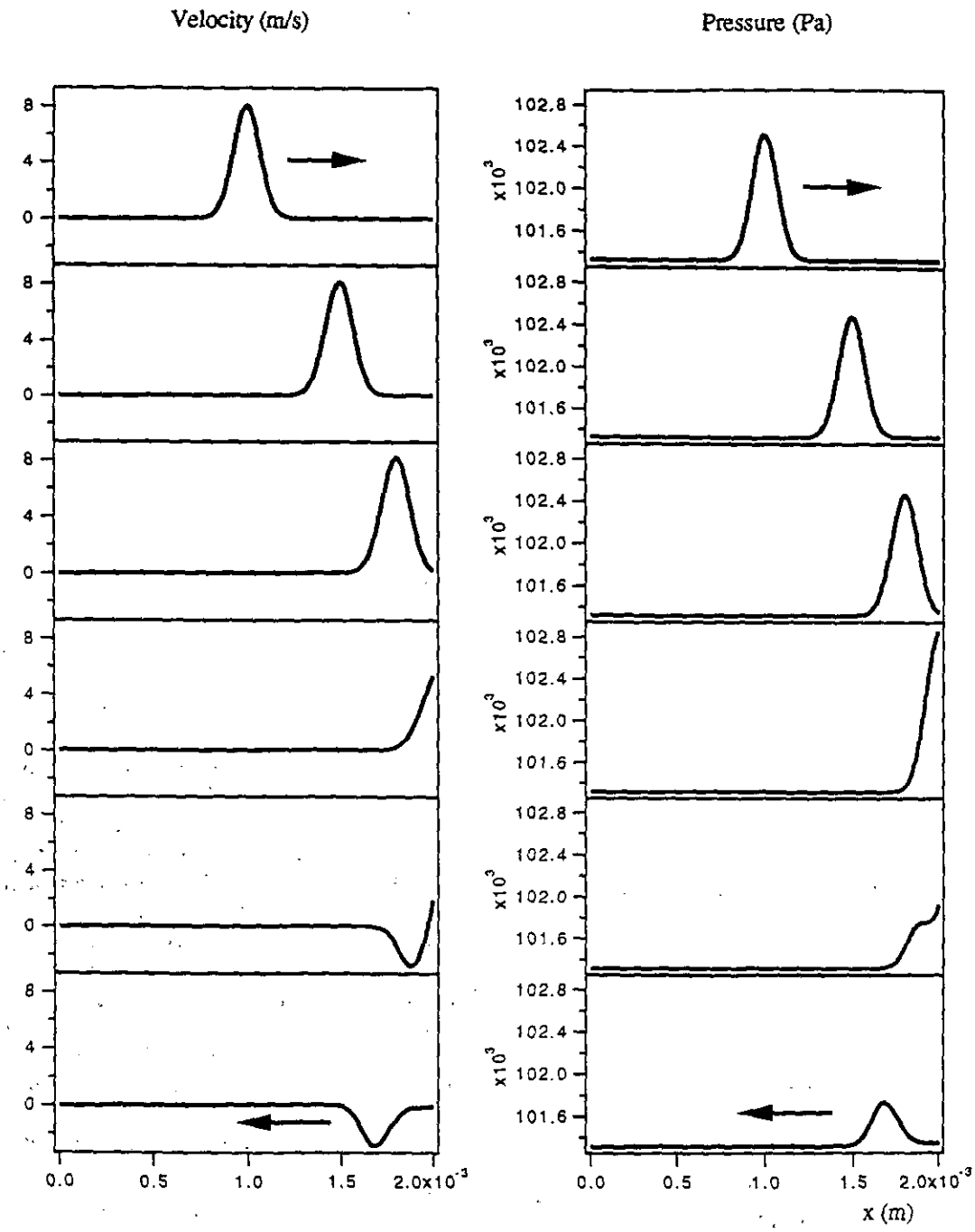

FIG. 1. Propagation of an acoustic wave towards a non-reflecting boundary with the previous method of Poinsot and Lele [1].

K is a constant which determines the speed with which the average pressure in the computational domain relaxes towards the imposed pressure at infinity p_∞. Rudy and Strikwerda [13, 14] suggest that the optimum value of K is of the order of $(1 - M^2)c/(2\rho\overline{C}_p L)$, where M is the maximal Mach number in the domain and L is a characteristic size of this domain. The vector $\mathcal{L}_1$ being the only free parameter, all the other $\mathcal{L}_i$'s are directly computed using (7) to (12).

The above local one-dimensional system present, of course, some imperfections for multidimensional cases, as pointed out in [1]. As we consider only a one-dimensional system at the boundary, this treatment is only exact for waves propagating perpendicularly to the boundaries of the domain, which leads to some small amount of reflections for other waves. In the same way, diffusion and reaction terms are only considered as being passively convected information. Nevertheless, numerous

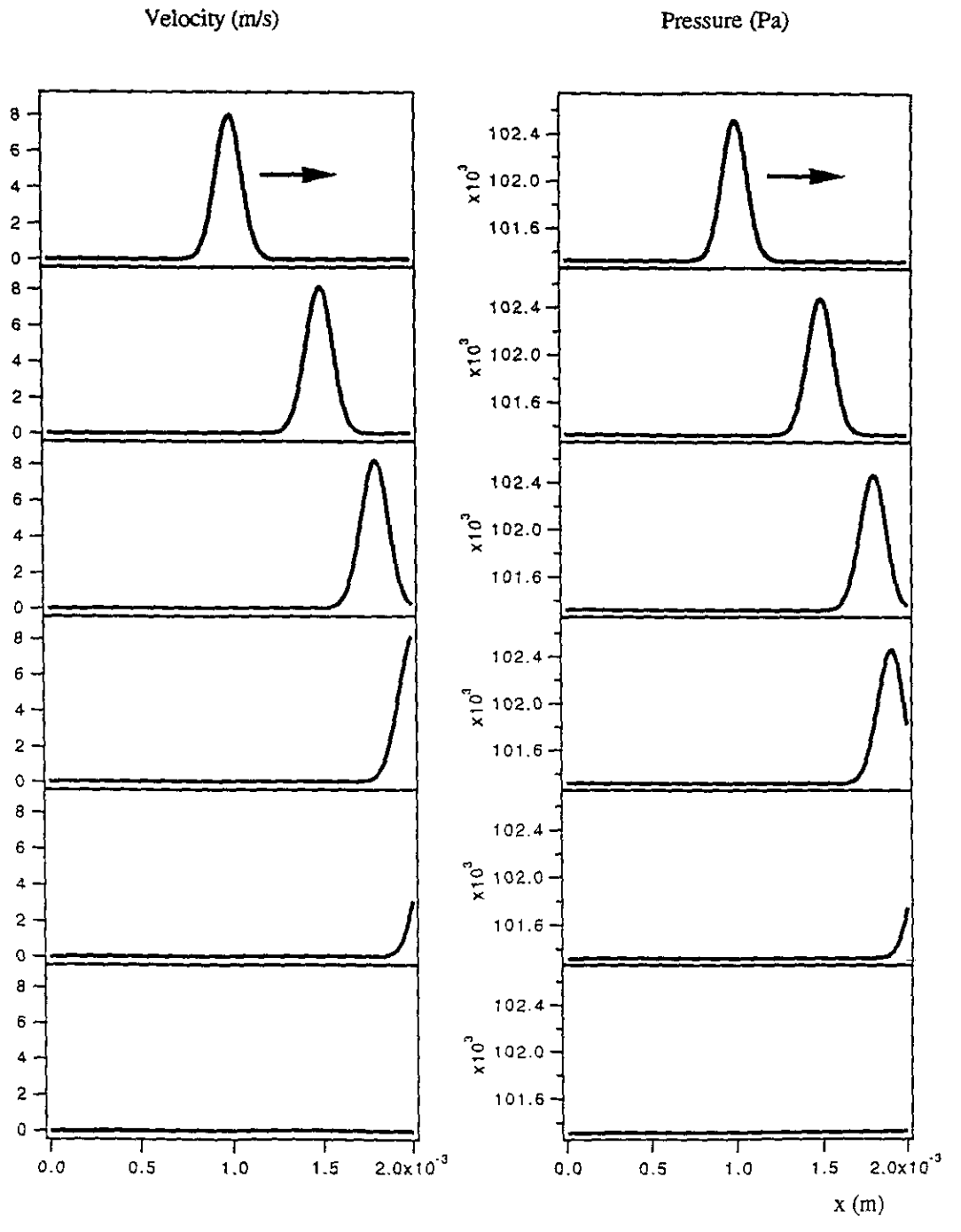

FIG. 2. Propagation of an acoustic wave towards a non-reflecting boundary with extended method.

computations have been conducted using, in particular, the non-reflecting and inlet-type conditions described above, but also isothermal or adiabatic wall conditions, as well as supersonic inflows and outflows [1–3, 15–18]. In all cases, the behavior of these boundary conditions has been the one expected, with a negligible amount of reflection at the boundaries, as can be seen from the examples proposed in the next section.

4. EXAMPLES OF APPLICATION

In order to test the improvements introduced by this new formulation over the previous one, we consider the behavior of acoustic and entropy waves at reflecting and non-reflecting boundaries. A summary of these different one-dimensional cases is proposed in Table I. The comptuational code used for these tests is a fully explicit direct simulation code solving

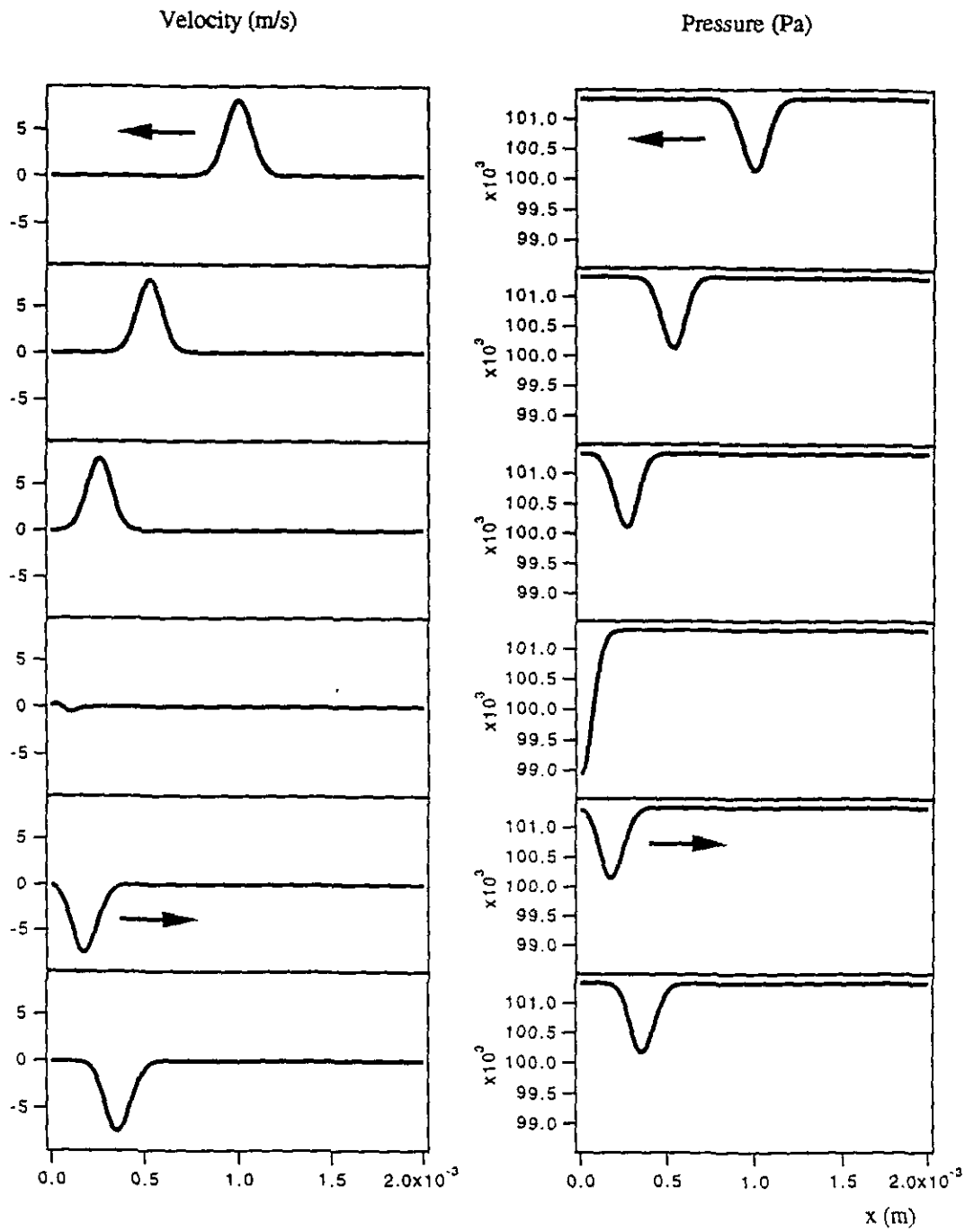

FIG. 3. Propagation of an acoustic wave towards an inlet-type boundary with extended method.

the complete reactive Navier–Stokes equation, using the CHEMKIN and TRANSPORT packages [10, 11] to model the influence of reacting gases with accurate thermodynamic coefficients [16]. This code has high-order accuracy (presently sixth order in space and third order in time). Spatial differencing is performed using compact schemes as described by Lele [19], while time differencing uses a third-order Runge–Kutta scheme.

A set of propagating acoustic waves is created at $t = 0$ by using the initial conditions

$$u = u_0 + \mathcal{A} \exp\left[-\left(\mathcal{B} \frac{x - L/2}{L} \right)^2 \right]$$

$$p = p_0 \pm \rho_0 c_0 (u - u_0)$$

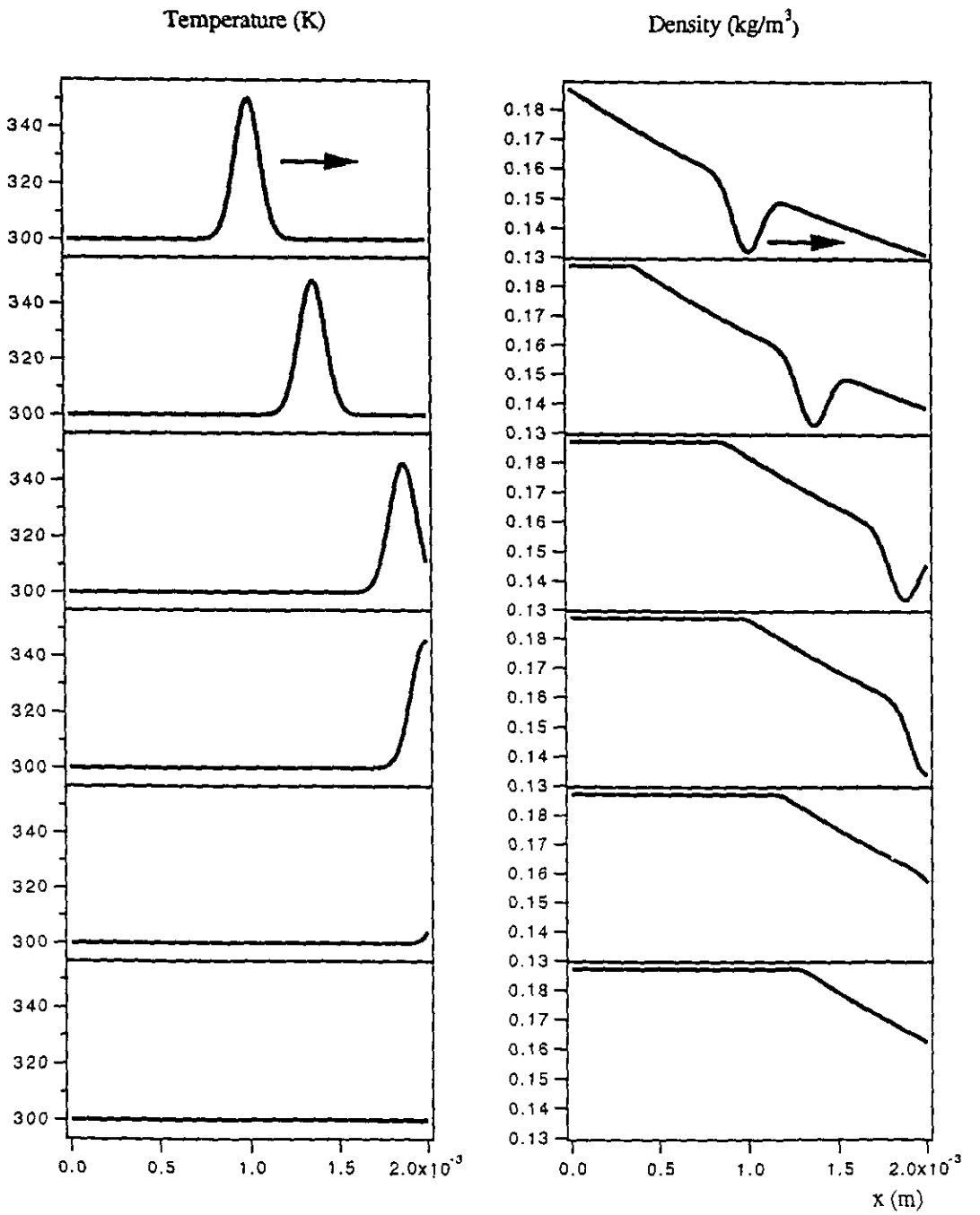

FIG. 4. Propagation of an entropy wave towards a non-reflecting boundary with extended method.

$$\rho = \rho_0 \pm \frac{\rho_0(u - u_0)}{c_0} \tag{27}$$

$$T = \frac{p}{\rho r},$$

where values with index 0 denote some original uniform state and $\mathcal{A}$ and $\mathcal{B}$ determine the strength and stiffness of the superimposed acoustic wave. The choice of the sign in the equations for p and ρ determines the direction in which the acoustic wave will propagate. Entropy waves correspond simply to a bulge in temperature (and the corresponding bulge in density) on an initial uniform field of velocity, density, pressure, and temperature. They propagate at the convection speed towards the chosen boundary.

The procedure of Poinsot and Lele was proven to be adequate in perfect gas cases with constant homogeneous thermodynamic properties [1], and we do not reproduce these results here.

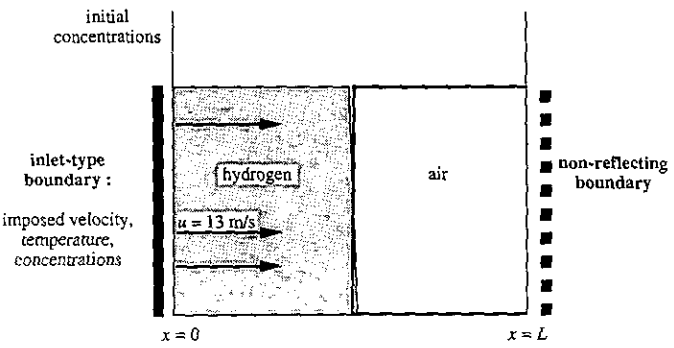

FIG. 5. Initial and boundary conditions corresponding to Figs. 6 to 9.

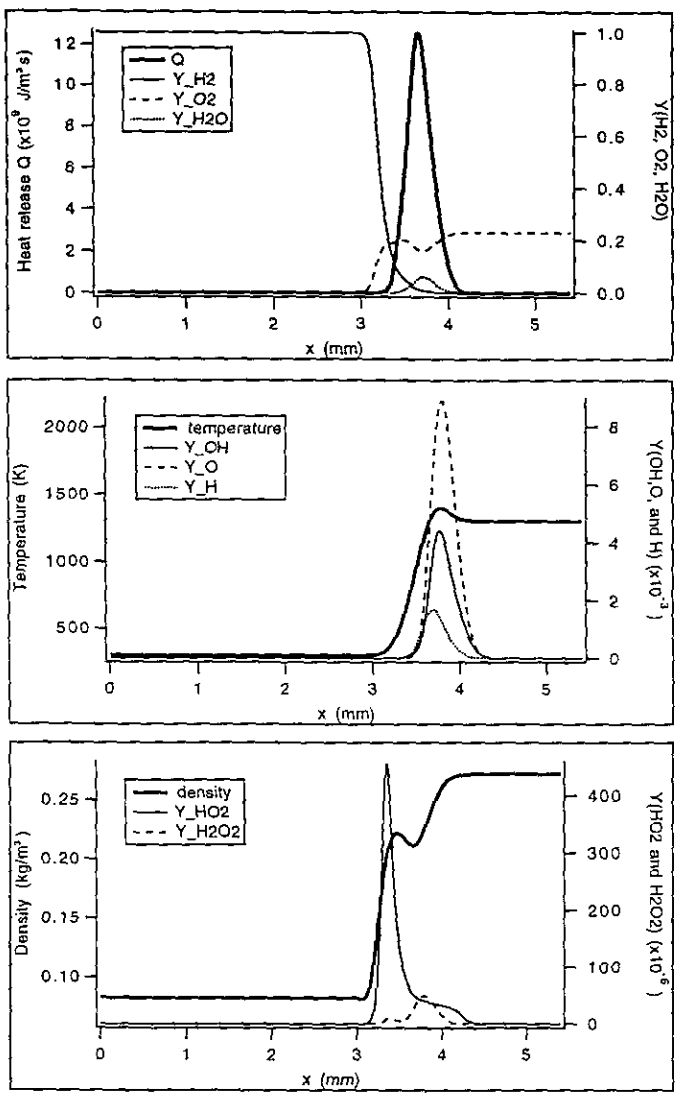

FIG. 6. Propagation of an igniting flame towards a non-reflecting boundary with extended method. Time $t = 5 \times 10^{-5}$ s.

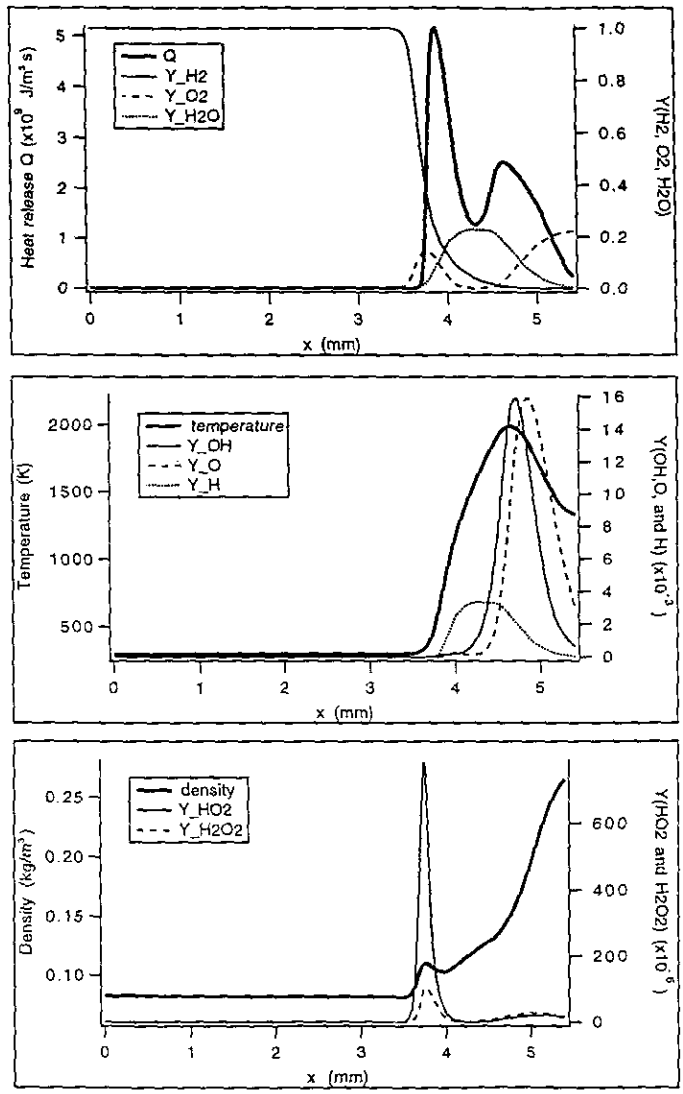

FIG. 7. Propagation of an igniting flame towards a non-reflecting boundary with extended method. Time $t = 9 \times 10^{-5}$ s.

In order to test the capacities of the extended technique, we work now with multicomponent inhomogeneous flows. In the first case of interest, an acoustic wave propagates towards the right boundary in a mixture of hydrogen and oxygen, where chemical reaction is not allowed. The two species concentrations present a constant gradient in the domain, with the initial conditions:

$$Y(H_2)_{x=0} = 0.4, \quad Y(H_2)_{x=L} = 0.6,$$
$$Y(O_2)_{x=0} = 0.6, \quad Y(O_2)_{x=L} = 0.4. \tag{28}$$

The right boundary is in this case a non-reflecting boundary with a constant $K = 0$. Although unadapted in most cases as explained in Section 3, this value of K can be chosen without problems for short-time simulations. This is, of course, the only value which gives a perfectly non-reflecting boundary. Taking

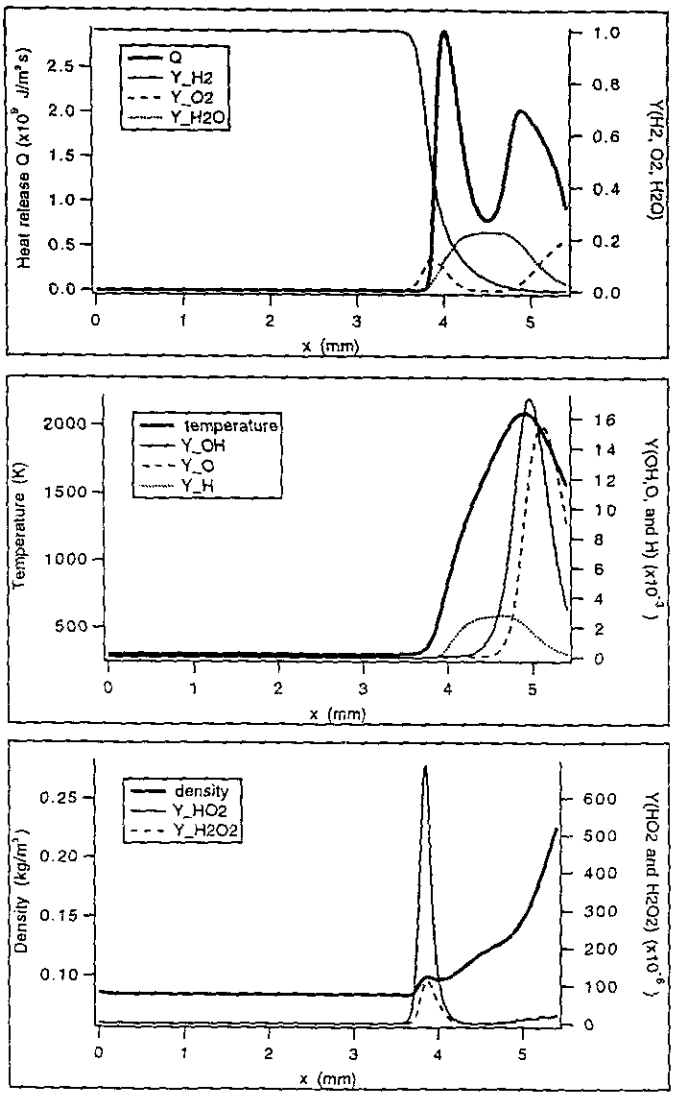

FIG. 8. Propagation of an igniting flame towards a non-reflecting boundary with extended method. Time $t = 1.1 \times 10^{-4}$ s.

$K > 0$ produces a partial reflection of the acoustic wave at the boundary, growing with K.

Using detailed thermodynamic models for the original formulation of the boundary conditions given in [1], the propagation of this acoustic wave is shown in Fig. 1. A non-negligible amount of numerical reflection can be seen when the acoustic wave comes in contact with the right boundary, which should in fact be perfectly "non-reflecting." The amplitude of this non-physical perturbation is such that this original formulation of the boundary treatment appears to be inappropriate when using realistic thermodynamic properties. It is in this case impossible to get accurate boundary conditions without taking into account the temperature and composition dependances of the gas properties.

The extended method described in this paper is able to deal with this problem (Fig. 2) and lets the acoustic wave go freely through the boundary. No reflection of the incoming acoustic wave can be seen at the right boundary.

In the second case, the same acoustic wave is propagating towards the left, and the left boundary is an inlet boundary with imposed values of velocity, temperature, energy, and concentrations. As in the above case, the extended method gives an oscillation-free exact result (Fig. 3), corresponding to the total reflection of the incoming wave.

The third case is analogous to the first one, but uses an entropy wave in the place of an acoustic wave. Once again, the new treatment appears to be particularly accurate, the entropy wave being convected without perturbation through the non-reflecting boundary (Fig. 4).

The fourth and last case corresponds to a situation studied in detail in [16]. In this problem, a one-dimensional hydrogen–air diffusion flame autoignites in the computational domain. Initial and boundary conditions are described in Fig. 5. Impos-

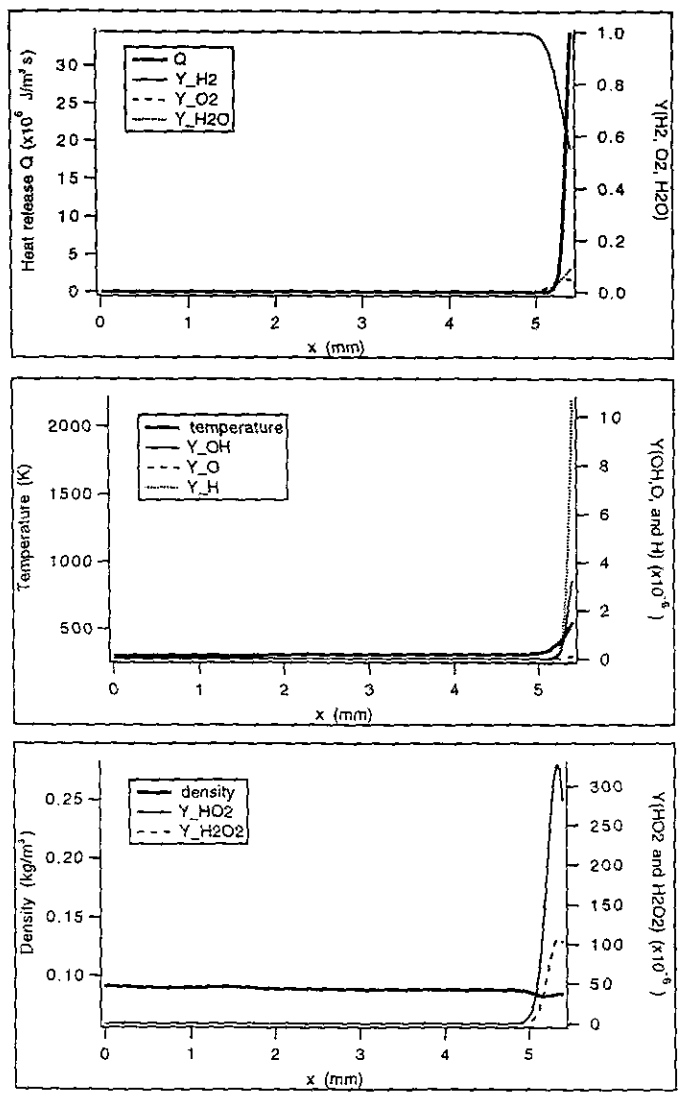

FIG. 9. Propagation of an igniting flame towards a non-reflecting boundary with extended method. Time $t = 2.5 \times 10^{-4}$ s.

ing as the initial and left-boundary condition a constant velocity, this igniting flame is pushed towards the right boundary, at which a non-reflecting condition with $K = 0.2$ is imposed. As can be seen in Figs. 6–9 corresponding to different physical times, the reacting flow passes through the boundary without perturbation. The evolution of the diffusion flame, which separates into two parts after the ignition [20, 21] is not perturbated by the crossing of the non-reflecting boundary. Such a test is particularly difficult for any type of boundary conditions, and, to the author's knowledge, very few boundary treatments allow an exact and oscillation-free result as observed here.

5. CONCLUDING REMARKS

The formulation of the boundary treatment based on characteristic wave relations, as proposed by Poinsot and Lele and extended in this paper for gases with realistic thermodynamic and reactive properties, appears to be particularly accurate and stable, as proved by the different tests presented in the previous section. This boundary formulation is very attractive for all direct simulations of turbulent reacting flows.

The method used in this paper is described in a three-dimensional case, and the examples of Section 4 are computed with a totally explicit finite-difference direct simulation code. But it must also be mentioned that this same boundary treatment has been implemented and is presently used in two-dimensional codes (planar or axisymmetric) and has also been used successfully in implicit solvers [22]. Deriving the adapted formulation for these latter cases from the basic one proposed in Section 2 was straightforward, and it is believed that the boundary formulation proposed here can be easily used in most cases of interest.

The treatment of the viscous terms at the boundaries is still in a transition phase, as they are up to now considered to be only passively convected with the flow. A complete formulation that takes thoroughly into consideration all terms in a similar way is presently under study.

APPENDIX A: CONSERVATIVE SYSTEM AND WAVE EXPRESSION AT THE BOUNDARIES

The mathematical treatment is given here for a three-dimensional problem, but its reduction to two-dimensional or axisymmetric cases is straightforward. For a multicomponent dimensional reactive mixture with N_s species, the system of conservative variables can be written

$$\begin{aligned}\tilde{U} &= (\tilde{U}_1, ..., \tilde{U}_{N_s+5})^t \\ &= (\rho, e_t, \rho u, \rho v, \rho w, \rho Y_1, ..., \rho Y_{N_s})^t.\end{aligned} \tag{A.1}$$

The primitive variables, chosen in order to get the most practical presentation, are taken as

$$\begin{aligned}U &= (U_1, ..., U_{N_s+5})^t \\ &= (\rho, T, u, v, w, Y_1, ..., Y_{N_s})^t.\end{aligned} \tag{A.2}$$

The matrix relating the system $\tilde{U}$, used to integrate the equations, to the system U in which we realize the analysis at the boundaries, is then

$$P = \partial\tilde{U}/\partial U \tag{A.3}$$

which, in our case, can be written

$$P = \begin{pmatrix}
1 & 0 & 0 & 0 & 0 & 0 & 0 & \cdots & \cdots & 0 \\
P_{2,1} & P_{2,2} & \rho u & \rho v & \rho w & P_{2,6} & P_{2,7} & \cdots & \cdots & P_{2,N_s+5} \\
u & 0 & \rho & 0 & 0 & 0 & 0 & \cdots & \cdots & 0 \\
v & 0 & 0 & \rho & 0 & 0 & 0 & \cdots & \cdots & 0 \\
w & 0 & 0 & 0 & \rho & 0 & 0 & \cdots & \cdots & 0 \\
Y_1 & 0 & 0 & 0 & 0 & \rho & 0 & \cdots & \cdots & 0 \\
Y_2 & 0 & 0 & 0 & 0 & 0 & \rho & 0 & \cdots & 0 \\
\vdots & \vdots & \vdots & \vdots & \vdots & \vdots & \ddots & \ddots & \ddots & \vdots \\
\vdots & 0 & 0 & 0 & 0 & 0 & \cdots & 0 & \rho & 0 \\
Y_{N_s} & 0 & 0 & 0 & 0 & 0 & 0 & \cdots & 0 & \rho
\end{pmatrix} \tag{A.4}$$

with, for i between 1 and N_s:

$$P_{2,1} = \frac{u^2 + v^2 + w^2}{2} + \sum_{i=1}^{N_s} (h_i Y_i) - \frac{RT}{\overline{W}} \tag{A.5}$$

$$P_{2,2} = \rho \overline{C}_v \tag{A.6}$$

$$P_{2,5+i} = \rho\left(h_i - \frac{RT}{W_i}\right). \tag{A.7}$$

The inverse matrix P^{-1} is then given by

$$\begin{pmatrix} 1 & 0 & 0 & 0 & 0 & 0 & \cdots & \cdots & 0 \\ P_{2,1}^{(-1)} & \dfrac{1}{\overline{\rho C_v}} & \dfrac{-u}{\overline{\rho C_v}} & \dfrac{-v}{\overline{\rho C_v}} & \dfrac{-w}{\overline{\rho C_v}} & P_{2,6}^{(-1)} & \cdots & \cdots & P_{2,N_s+5}^{(-1)} \\ -u/\rho & 0 & 1/\rho & 0 & 0 & 0 & \cdots & \cdots & 0 \\ -v/\rho & 0 & 0 & 1/\rho & 0 & 0 & \cdots & \cdots & 0 \\ -w/\rho & 0 & 0 & 0 & 1/\rho & 0 & \cdots & \cdots & 0 \\ -Y_1/\rho & 0 & 0 & 0 & 0 & 1/\rho & 0 & \cdots & 0 \\ \vdots & 0 & \vdots & \vdots & \vdots & 0 & \ddots & \ddots & \vdots \\ \vdots & 0 & 0 & 0 & 0 & 0 & 0 & 1/\rho & 0 \\ -Y_{N_s}/\rho & 0 & 0 & 0 & 0 & 0 & 0 & 0 & 1/\rho \end{pmatrix} \tag{A.8}$$

with

$$P_{2,1}^{(-1)} = \frac{u^2 + v^2 + w^2}{2\overline{\rho C_v}} \tag{A.9}$$

$$P_{2,5+i}^{(-1)} = \frac{(RT/W_i) - h_i}{\overline{\rho C_v}} \quad (i = 1\text{–}N_s). \tag{A.10}$$

Defining as F^k the flux vector of the conservative variables along the kth direction, one gets, for example, in the x direction:

$$F^1 = (F_1^1, \ldots, F_{N_s+5}^1)' \tag{A.11}$$

$$= (\rho u, (e_t + p)u, \rho u^2 + p, \rho uv, \rho uv, \rho uY_1, \ldots, \rho uY_{N_s})'.$$

It is then possible to write

$$\frac{\partial F^k}{\partial x_k} = Q^k \frac{\partial U}{\partial x_k}, \tag{A.12}$$

where the matrix Q^k is composed of elements q_{ij}^k:

$$q_{ij}^k = \partial F_i^k / \partial U_j. \tag{A.13}$$

In our case, Q^1 is simply written

$$\begin{pmatrix} u & 0 & \rho & 0 & 0 & 0 & \cdots & \cdots & 0 \\ Q_{2,1}^1 & \rho u\overline{C_p} & Q_{2,3}^1 & \rho uv & \rho uw & \rho uh_1 & \cdots & \cdots & \rho uh_{N_s} \\ \dfrac{RT}{\overline{W}} + u^2 & \dfrac{\rho R}{\overline{W}} & 2\rho u & 0 & 0 & \dfrac{\rho RT}{W_1} & \cdots & \cdots & \dfrac{\rho RT}{W_{N_s}} \\ uv & 0 & \rho v & \rho u & 0 & 0 & \cdots & \cdots & 0 \\ uw & 0 & \rho w & 0 & \rho u & 0 & \cdots & \cdots & 0 \\ uY_1 & 0 & \rho Y_1 & 0 & 0 & \rho u & 0 & \cdots & 0 \\ \vdots & \vdots & \vdots & \vdots & \vdots & 0 & \ddots & \ddots & \vdots \\ uY_{N_s-1} & 0 & \rho Y_{N_s-1} & 0 & 0 & 0 & 0 & \rho u & 0 \\ uY_{N_s} & 0 & \rho Y_{N_s} & 0 & 0 & 0 & \cdots & 0 & \rho u \end{pmatrix} \tag{A.14}$$

with

$$Q_{2,1}^1 = u\left(\frac{u^2 + v^2 + w^2}{2} + \sum_{i=1}^{N_s} h_i Y_i\right) \tag{A.15}$$

$$Q_{2,3}^1 = \rho\left(\frac{u^2 + v^2 + w^2}{2} + u^2 + \sum_{i=1}^{N_s} h_i Y_i\right). \tag{A.16}$$

If one considers now the x boundaries (the formulation being symmetrical for the y and z boundaries), the system of equations can be written in conservative form:

$$\frac{\partial \tilde{U}}{\partial t} + \frac{\partial F^1}{\partial x} + \tilde{C} = 0. \tag{A.17}$$

The vector $\tilde{C}$ includes all terms which do not contain any

first derivative of $\tilde{U}$ along the x direction. These terms are considered as being passively convected along the x direction and do not play a role in the present characteristic wave analysis. The vector $\tilde{C}$ stands here also for all diffusive derivatives and reactive source terms.

Defining

$$A^k = P^{-1}Q^k, \tag{A.18}$$

Eq. (A.17) can be cast into primitive form, according to

$$\frac{\partial U}{\partial t} + A^1 \frac{\partial U}{\partial x} + C = 0. \tag{A.19}$$

The matrix A^1 is then given by

$$\begin{pmatrix}
u & 0 & \rho & 0 & 0 & 0 & 0 & \cdots & 0 \\
0 & u & \dfrac{RT}{\overline{C_v}\,\overline{W}} & 0 & 0 & 0 & 0 & \cdots & 0 \\
\dfrac{RT}{\rho\overline{W}} & \dfrac{R}{\overline{W}} & u & 0 & 0 & \dfrac{RT}{\overline{W}_1} & \dfrac{RT}{\overline{W}_2} & \cdots & \dfrac{RT}{\overline{W}_{N_s}} \\
0 & 0 & 0 & u & 0 & 0 & 0 & \cdots & 0 \\
0 & 0 & 0 & 0 & u & 0 & 0 & \cdots & 0 \\
0 & 0 & 0 & 0 & 0 & u & 0 & \cdots & 0 \\
\vdots & \vdots & \vdots & \vdots & \vdots & \ddots & \ddots & \ddots & \vdots \\
\vdots & 0 & 0 & 0 & 0 & \cdots & 0 & u & 0 \\
0 & 0 & 0 & 0 & 0 & 0 & \cdots & 0 & u
\end{pmatrix}. \tag{A.20}$$

Writing the determinant of $(A - \lambda I)$, one can easily find the $N_s + 5$ eigenvalues of matrix A:

$$\begin{aligned}
\lambda_1 &= u - c \\
\lambda_2 &= u \\
&\vdots \\
\lambda_{N_s+4} &= u \\
\lambda_{N_s+5} &= u + c.
\end{aligned} \tag{A.21}$$

Note that eigenvalues λ_2 to λ_{N_s+4} are identical and equal to the local velocity u. A base of right eigenvectors, associated with the above eigenvalues, is given for example by, for $i = N_s$,

$$\begin{aligned}
r_1 &= \left(\frac{\rho\overline{C_p}}{c^2}, 1, -\frac{\overline{C_p}}{c}, 0, 0, 0, 0, 0, ..., 0\right)^t \\
r_2 &= (0, 0, 0, 1, 0, 0, 0, 0, ..., 0)^t \\
r_3 &= (0, 0, 0, 0, 1, 0, 0, 0, ..., 0)^t \\
r_{i+3} &= (0, 1, 0, ..., 0, \underbrace{-\frac{W_i}{\overline{W}\overline{T}}}_{\text{index } i+5}, 0, ..., 0)^t \\
r_{N_s+4} &= (1, 0, 0, 0, 0, -\frac{W_1}{\rho\overline{W}}, 0, 0, ..., 0)^t \\
r_{N_s+5} &= \left(\frac{\rho\overline{C_p}}{c^2}, 1, \frac{\overline{C_p}}{c}, 0, 0, 0, 0, 0, ..., 0\right)^t.
\end{aligned} \tag{A.22}$$

It is then possible to constitute a matrix S by taking as columns the eigenvectors r_k given by (A.22). Inverting S gives a base of *left* eigenvectors l_i, which can be cast in the form, for i between 2 and N_s,

$$\begin{aligned}
l_1 &= \left(\frac{\gamma-1}{2\gamma}\frac{T}{\rho}, \frac{\gamma-1}{2\gamma}, -\frac{c}{2\overline{C_p}}, 0, 0, \frac{\gamma-1}{2\gamma}\frac{\overline{W}T}{W_1}, ..., \frac{\gamma-1}{2\gamma}\frac{\overline{W}T}{W_{N_s}}\right) \\
l_2 &= (0, 0, 0, 1, 0, 0, 0, 0, ..., 0) \\
l_3 &= (0, 0, 0, 0, 1, 0, 0, 0, ..., 0) \\
l_4 &= \left(\frac{1-\gamma}{\gamma}\frac{T}{\rho}, \frac{1}{\gamma}, 0, 0, 0, \frac{1-\gamma}{\gamma}\frac{\overline{W}T}{W_1}, \frac{\overline{W}T}{\gamma W_2}, ..., \frac{\overline{W}T}{\gamma W_{N_s}}\right) \\
l_{i+3} &= (0, 0, 0, ..., 0, \underbrace{-\frac{\overline{W}T}{W_i}}_{\text{index } i+5}, 0, ..., 0) \\
l_{N_s+4} &= \left(\frac{\gamma-1}{\gamma}, -\frac{\rho}{\gamma T}, 0, 0, 0, -\frac{\rho\overline{W}}{\gamma W_1}, ..., -\frac{\rho\overline{W}}{\gamma W_{N_s}}\right) \\
l_{N_s+5} &= \left(\frac{\gamma-1}{2\gamma}\frac{T}{\rho}, \frac{\gamma-1}{2\gamma}, \frac{c}{2\overline{C_p}}, 0, 0, \frac{\gamma-1}{2\gamma}\frac{\overline{W}T}{W_1}, ..., \frac{\gamma-1}{2\gamma}\frac{\overline{W}T}{W_{N_s}}\right).
\end{aligned} \tag{A.23}$$

The vector l_1 is associated to the eigenvalue $(u - c)$, l_{N_s+5} to $(u + c)$, l_2 to l_{N_s+4} are all associated to the eigenvalue u. The l_1 and l_{N_s+5} waves correspond to acoustic waves while all the others are convected by the mean flow. For $i = 1$ to $(N_s + 5)$, one can define the vector $\mathcal{L}$ of components $\mathcal{L}_i$, representing the wave amplitude variations:

$$\mathcal{L}_i = \lambda_i l_i \frac{\partial U}{\partial x}. \tag{A.24}$$

Using $\mathcal{L}$, Eq. (A.19) can also be written

$$\frac{\partial U}{\partial t} + S\mathcal{L} + C = 0, \tag{A.25}$$

or in conservative form,

$$\frac{\partial \tilde{U}}{\partial t} + PS\mathcal{L} + \tilde{C} = 0. \tag{A.26}$$

The values of the components of vector $\mathcal{L}$ are proposed in Eqs. (6) to (12). Using these equations, the vector $S\mathcal{L}$ representing the convective terms of the primitive system is

$$S\mathcal{L} = \begin{cases} (\rho\overline{C}_p/c^2)(\mathcal{L}_1 + \mathcal{L}_{N_s+5}) + \mathcal{L}_{N_s+4} \\ \mathcal{L}_1 + \mathcal{L}_{N_s+5} + \sum_{i=4}^{N_s+3} \mathcal{L}_i \\ (\mathcal{L}_{N_s+5} - \mathcal{L}_1)\overline{C}_p/c \\ \mathcal{L}_2 \\ \mathcal{L}_3 \\ -W_1\mathcal{L}_4/)\overline{WT}) - W_1\mathcal{L}_{N_s+4}/(\overline{W}\rho) \\ -W_2\mathcal{L}_5/(\overline{WT}) \\ \vdots \\ -W_{N_s}\mathcal{L}_{N_s+3}/(\overline{WT}). \end{cases} \tag{A.27}$$

APPENDIX B: LIST OF SYMBOLS

$\mathcal{A}$, $\mathcal{B}$	parameters for the acoustic wave definition
A	reduced matrix for the convective term coefficients
c	sound velocity (m/s)
$\overline{C}_p$	heat capacity of the mixture at constant pressure (J/(kg.K))
$\overline{C}_v$	heat capacity of the mixture at constant volume (J/(kg.K))
C	viscous, transverse and reactive terms in the primitive system
$\tilde{C}$	viscous, transverse and reactive terms in the conservative system
e_t	total energy (J/m^3)
F^k	flux vector of the conservative variables along direction k
γ	C_p/C_v (−)
h_i	enthalpy of species i (J/kg)
h_t	total enthalpy $(e_t + p)/\rho$ (J/kg)
K	pressure relaxation constant (1/s)
L	length of the domain (m)
l_i	ith left eigenvector of matrix A
$\mathcal{L}_i$	ith wave amplitude variation associated to the primitive system
λ_i	ith eigenvalue of matrix A, associated to wave $\mathcal{L}_i$ (m/s)
M	Mach number (−)
N_s	number of chemical species considered (−)
P	transformation matrix between $\tilde{U}$ and U
p	pressure (Pa)
q_i	ith component of the heat flux (kg/s^3)
R	gas constant (J/mol.K))
r	$R/\overline{W}$ (J/(kg.K))
r_i	ith right eigenvector of matrix A
ρ	density (kg/m^3)
τ_{ij}	i, j component of stress tensor (Pa)
u, v, w	velocity along x, y, and z (m/s)
u_i	velocity along x_i (m/s)
U, $\tilde{U}$	vectors of primitive and conservative variables
Y_i	mass fraction of species i (−)
$V_{Di,j}$	diffusion velocity of species i along direction j (m/s)
$\overline{W}$	mean molar mass (kg/mol)
W_i	molar mass of species i (kg/mol)
$\dot{\omega}_i$	chemical production rate of species i (mol/(m^{3}s)).

ACKNOWLEDGMENTS

The authors wish to acknowledge the support of SNECMA and of the European Community. Many helpful discussions with J. Segatz must also be mentioned.

REFERENCES

1. T. J. Poinsot and S. K. Lele, *J. Comput. Phys.* **101,** 104 (1992).
2. S. K. Lele, "27th Aerospace Sciences Meeting, 1989," AIAA Paper 89-0374 (unpublished).
3. T. Poinsot, D. Veynante, and S. Candel, *J. Fluid Mech.* **228,** 561 (1991).
4. K. W. Thompson *J. Comput. Phys.* **68,** 1 (1987).
5. J. C. Strikwerda, *Commun. Pure Appl. Math.* **30,** 797 (1977).
6. P. Dutt, *SIAM J. Numer. Anal.* **25**(2), 245 (1988).
7. R. Vichnevetsky and J. B. Bowles, *Fourier Analysis of Numerical Approximations of Hyperbolic Equations,"* (SIAM, Philadelphia, 1982).
8. T. C. Vanajakshi, K. W. Thompson, and D. C. Black, *J. Comput. Phys.* **84,** 343 (1989).
9. K. W. Thompson, "Stanford Summer Program, 1990" (unpublished).
10. R. J. Kee, J. A. Miller, and T. H. Jefferson, SANDIA Rep. SAND80-8003, 1980 (unpublished).
11. R. J. Kee, J. Warnatz, and J. A. Miller, SANDIA Rep. SAND83-8209, 1983 (unpublished).
12. F. A. Williams, "Combustion Theory," 2nd ed., (Addison–Wesley, Reading, MA, 1985).
13. D. H. Rudy and J. C. Strikwerda, *J. Comput. Phys.* **36,** 55 (1980).
14. D. H. Rudy and J. C. Strikwerda, *Comput. & Fluids* **9,** 327 (1981).
15. T. Poinsot, D. Veynante, and S. Candel, in *Proceedings, Twenty-third Symposium (International) on Combustion, 1990* (The Combustion Institute, Pittsburgh, 1990).
16. D. Thévenin, "Dynamique de l'allumage de flammes de diffusion dans des écoulements cisaillés," Thèse de doctorat, Ecole Centrale Paris, Nbr. 92-042, 1992 (unpublished).
17. D. Thévenin, F. Behrendt, U. Maas, and J. Warnatz, in *Proceedings, Fifth International Conference on Numerical Combustion, Garmisch-Partenkirchen, Germany, 1993,* p. 121 (unpublished).
18. M. Baum, T. J. Poinsot, and D. C. Haworth, in *Proceedings, Fifth International Conference on Numerical Combustion, Garmisch-Partenkirchen, Germany,* 1993, p. 18 (unpublished).
19. S. K. Lele, *J. Comput. Phys.* **103,** 16 (1992).
20. A. Liñan and A. Crespo, *Combust. Sci. Technol.* **14,** 95 (1976).
21. D. Thévenin and S. M. Candel, *Combust. Sci. Technol.* **91,** 73 (1993).
22. J. Segatz, U. Maas, R. Rannacher, J. Warnatz, and J. Wolfrum, in *Proceedings, Fifth International Conference on Numerical Combustion, Garmisch-Partenkirchen, Germany,* 1993, p. 110 (unpublished).